

Michael Doebeli

## A model for the evolutionary dynamics of cross-feeding polymorphisms in microorganisms

Received: February 19, 2002 / Accepted: May 8, 2002

**Abstract** Understanding mechanisms of evolutionary diversification is central to evolutionary biology. Microbes constitute promising model systems for observing processes of diversification directly in the laboratory. One of the main existing paradigms for microbial diversification is the evolution of cross-feeding polymorphisms, in which a strain specializing on a primary resource coexists with a cross-feeding strain that specializes on a waste product resulting from consumption of the primary resource. Here I propose a theoretical model for the evolutionary dynamics through which cross-feeding polymorphisms can gradually emerge from a single ancestral strain. The model is based on the framework of adaptive dynamics, which has proved to be very useful for studying adaptive processes of divergence under sympatric conditions. In particular, the phenomenon of evolutionary branching serves as a general paradigm for diversification. I show that evolutionary branching naturally occurs in evolutionary models of cross-feeding if (1) there is a trade-off between uptake efficiencies on the primary and secondary resources, and (2) this trade-off has positive curvature. The model also suggests that the evolution of cross-feeding should be more likely in chemostat cultures than in serial batch cultures, which conforms with empirical observations. Overall, the model provides a theoretical metaphor for the evolution of cross-feeding polymorphisms.

**Key words** Crossfeeding · Polymorphism · Adaptive dynamics · Evolutionary branching · Tradeoff · Frequency dependence

### Introduction

Understanding the origin and evolution of diversity is one of the central problems in population biology. In particular, understanding the processes of speciation is of fundamental importance. Although traditional discussions of speciation are based on geographic patterns of species distributions (Mayr 1963; Turelli et al. 2001), recent theoretical developments have studied the ecological mechanisms that can drive adaptive divergence between different lineages (Geritz et al. 1998; Dieckmann and Doebeli 1999; Doebeli and Dieckmann 2000). In this context, the phenomenon of evolutionary branching is of particular importance. During this evolutionary process, frequency-dependent selection drives an evolving lineage to a point in phenotype space where selection turns disruptive, after which the lineage splits into two diverging phenotypic branches. Evolutionary branching is a paradigm for evolutionary diversification emerging from the theoretical framework of adaptive dynamics (Metz et al. 1996; Dieckmann and Law 1996; Geritz et al. 1998). The main conceptual idea underlying this theory for evolutionary dynamics is that the phenotypic distribution of a resident population, as well as its ecological dynamics, are important determinants of the environment that a mutant phenotype encounters when it first appears in the population. This intuitively appealing idea is captured in the notion of the invasion fitness, which describes how the long-term growth rate of a rare mutant depends on the resident phenotypes. Roughly speaking, adaptive dynamics is then derived as the gradient dynamics of the invasion fitness function, which yields, in its simplest interpretation, a theory for gradual evolutionary change in asexual populations. Although this asexual theory has already generated a number of interesting and useful theoretical results about general mechanisms of diversification (e.g. Doebeli and Ruxton 1997; Kisdi 1999; Geritz et al. 1999; Maire et al. 2001), models for evolutionary branching obviously must be extended with population genetics to be meaningful for diversification in sexual populations, i.e., for speciation. This has indeed been achieved (Dieckmann and Doebeli

M. Doebeli  
Departments of Zoology and Mathematics, University of British  
Columbia, 6270 University Blvd., Vancouver, BC, Canada V6T 1Z4  
Tel. +1-604-822-3326; Fax +1-604-822-2416  
e-mail: doebeli@zoology.ubc.ca

1999; Kisdi and Geritz 1999; Doebeli and Dieckmann 2000), leading to a general theory of adaptive speciation under sympatric conditions, i.e., speciation in the presence of gene flow and in the absence of geographic isolation.

The past years have seen a surge of empirical data suggesting that contrary to traditional views, speciation in the presence of gene flow is not an uncommon occurrence in nature (for pertaining recent reviews, see Turelli et al. 2001; Via 2001). However, even though there are some nice empirical examples of recent or ongoing adaptive divergence (Schluter 1994), possibly leading to speciation (Schlieven et al. 2001; Jiggins et al. 2001), many natural model systems tend to be inappropriate for experimental tests of speciation processes because generation times of the organisms involved, and hence the time scale of evolutionary change, are too long. There is an important exception to this, however: experimental evolution in microorganisms offers an escape from the conundrum of long generation times. Indeed, microorganisms appear to constitute very promising model systems for studying the evolution of diversity (Helling et al. 1987; Rosenzweig et al. 1994; Turner et al. 1996; Xu et al. 1996; Rainey and Travisano 1998; Treves et al. 1998; Travisano and Rainey 2000; Rozen and Lenski 2000; Kassen et al. 2000). For example, Rainey and Travisano (1998) found rapid evolution of phenotypically and genetically distinct lineages out of a single ancestral *Escherichia coli* lineage in spatially heterogeneous habitats.

The ecological mechanisms underlying the evolution and maintenance of this diversity are not yet well understood. However, it is clear that frequency-dependent selection plays an important role, because the various phenotypes tend to have positive growth rates when they are rare in an environment consisting of populations of the other phenotypes (Rainey and Travisano 1998). This is precisely the situation embodied by the invasion fitness function in adaptive dynamics, and it is particularly tempting to try to apply this theoretical framework to bacterial evolution because in many such systems the assumption of asexual reproduction appears to be largely satisfied.

One of the best understood cases of evolutionary diversification in bacteria is the evolution of a cross-feeding polymorphism in *E. coli* (Helling et al. 1987; Rosenzweig et al. 1994; Turner et al. 1996; Treves et al. 1998; Rozen and Lenski 2000). This process can be envisaged as follows: bacteria limited by a single nutrient, glucose, first evolve to become more efficient in glucose uptake. However, this increased efficiency comes at the expense of efficient uptake of secondary “waste” products, such as acetate, that are secreted during glucose metabolism. Therefore, mutants that are efficient metabolite consumers, but less efficient on the primary resource, can invade the system, leading to a polymorphism with one type being efficient in the uptake of the primary resource, and the other type being efficient at “cross-feeding” on the products resulting from the resource metabolism of the first type. This description is of course just a simplified caricature, and in reality the processes involved are rather intricate (Rosenzweig et al. 1994). In particular, cross-feeding on different metabo-

lites can lead to coexistence of different specialist and generalist cross-feeders (Rosenzweig et al. 1994; see also Dykhuizen and Davies 1980, for coexistence between generalist and specialist microbial strains).

It is intuitively clear that cross-feeding polymorphisms require the existence of trade-offs between uptake efficiencies on different nutrients. Such trade-offs could be the consequence of physiological constraints on catabolic pathways for different nutrients. Indeed, there is some empirical evidence that such trade-offs exist and that they are mediated by differential enzyme activities (Rosenzweig et al. 1994; Turner et al. 1996), which makes it likely that these trade-offs have a genetic basis; i.e., that for any given strain, its position on the trade-off curve is genetically determined. Although some distinct genetic differences between different strains constituting a glucose–acetate cross-feeding polymorphism have been suggested (Rosenzweig et al. 1994), it is reasonable to assume that genetic change along the trade-off curve is gradual because the metabolic pathways involved are rather complicated and can be affected in many different ways. This assumption is supported by the finding that a number of different morphs have been found in *E. coli* cross-feeding polymorphisms (Helling et al. 1987). Therefore, adaptive dynamics appears to be an appropriate theoretical framework for studying the evolution of cross-feeding.

The purpose of this article is to present a model for the gradual evolution of a cross-feeding polymorphism from a single ancestral lineage. The model is based on classical Michaelis–Menten dynamics for the uptake of a resource that is continually supplied in a chemostat. It is assumed that this primary resource is limiting, and that its consumption results in the production of a secondary nutrient as a metabolic waste product. A trade-off in uptake rates of the primary and secondary resource then results in frequency-dependent selection, because the fate of a mutant depends on the environment generated by the resident: if the resident is very efficient on the primary resource, it produces a lot of secondary metabolites, so that it may pay a mutant to be efficient on these secondary resources at the expense of primary efficiency; on the other hand, if the resident is not very efficient on the primary resource, then metabolites are not very abundant, and it may simply pay to be more efficient on the primary resource. I show, in the simple model presented, that this frequency dependence can lead to evolutionary branching, and hence to the gradual evolutionary split into two distinct strains, one a specialist on the primary resources, and the other a specialist on the secondary resource that is produced by the primary resource specialist.

By yielding a stable polymorphism the model also serves as a mathematical description of an example of coexistence of two different bacterial species on a single primary resource. It has long been known that microbial organisms can violate the ecological principle of competitive exclusion in a number of ways (Stewart and Levin 1973; Thingstad et al. 1996; Xu et al. 1996; see also references in Rosenzweig et al. 1994). Yomo et al. (1996) have introduced an interesting mathematical model for coexistence between two different microbial strains living in chemostats in which the bacteria

are provided with a single external resource. In their model, the external resource is metabolized by the bacteria into a secondary resource, and both resources are essential for bacterial growth. Yomo et al. (1996) showed that strains with different metabolic rate constants for synthesizing the secondary resource from the primary resource can coexist. The resulting polymorphism is similar to a cross-feeding polymorphism, except that in cross-feeding scenarios, it is usually only the primary resource that is limiting in the ancestral strain (i.e., the secondary metabolite is not essential for growth of the strain that is not cross-feeding).

In the model of Yomo et al. (1996), coexistence requires a certain degree of differentiation in the metabolic rate constants of the two competing strains. Even though it is reasonable to assume that single mutations affecting enzymatic activity could lead to a considerable change in metabolic rates, this model therefore does not describe an evolutionary process that is driven by mutations of arbitrarily small effects. In addition, Yomo et al. (1996) only considered competition between two given strains differing in their metabolic rates, and they did not address the question of how metabolic rates would change evolutionarily due to selection in each of the competing strains. In contrast, the model introduced here allows for arbitrarily small mutational effects, and for repeated occurrence of new mutations in the strains that are already present. In this way, the model shows how arbitrarily small phenotypic changes can lead to the gradual evolution of cross-feeding polymorphisms.

Perhaps the most widely cited theoretical description of microbial coexistence on a single resource is that by Stewart and Levin (1973), who show how a trade-off between growth rates at low and high concentration of a single resource can lead to coexistence of different types in serial batch cultures, i.e., in an environment in which the concentration of the resource changes temporally. In chemostat cultures, however, where the influx of the resource is constant, such a trade-off cannot lead to coexistence (Stewart and Levin 1973). Interestingly, when the model introduced here is modified to describe serial batch cultures rather than chemostats, the evolution of a cross-feeding polymorphism through a trade-off between uptake efficiencies on primary and secondary resources becomes much less likely. This result conforms with empirical data suggesting that cross-feeding polymorphisms in *E. coli* are less likely to evolve when the bacteria are propagated in batch cultures than when they are cultured in chemostats (Rozen and Lenski 2000; M. Travisano, personal communication).

## The model

Adaptive dynamics is based on calculations of the invasion fitness function for mutant phenotypes in the ecological environment generated by resident phenotypes. Therefore, the first step in formulating a model for the evolutionary dynamics of cross-feeding consists of setting up a model for the ecological dynamics of a monomorphic population con-

sisting of a single phenotype. Here I take this basic model to be a Michaelis–Menten type model for microbial growth in a chemostat culture. Let  $n(t)$  be the population density of the bacteria at time  $t$ , and let  $c(t)$  be the concentration of the primary resource, here glucose, in the chemostat at time  $t$ . The flow rate at which chemicals and organisms enter and leave the chemostat is denoted by  $d$ , so that in the absence of bacteria consuming the glucose, the rate of change in the glucose concentration in the chemostat is

$$\frac{dc}{dt} = -d \cdot c + d \cdot c_0 \quad (1)$$

where  $c_0$  is the glucose concentration in the ambient environment supplying the chemostat with glucose. If consumption of secondary metabolic waste products is neglected, so that growth of the bacterial population is only due to consumption of glucose, the rate of change of the population density is given by

$$\frac{dn}{dt} = \frac{r_g \cdot c}{k_g + c} \cdot n - d \cdot n \quad (2)$$

where  $r_g$  and  $k_g$  are parameters describing how the per capita bacterial growth rate changes with glucose concentration:  $r_g$  is the maximal per capita growth rate, whereas  $k_g$  is equal to that glucose concentration at which the per capita growth rate is  $r_g/2$ . Because of bacterial consumption, glucose concentration is decreased, so that the differential equation for the glucose concentration becomes

$$\frac{dc}{dt} = -\frac{1}{y_g} \frac{r_g \cdot c}{k_g + c} \cdot n - d \cdot c + d \cdot c_0 \quad (3)$$

where  $y_g$  is the “yield” (that is,  $y_g$  units of population increment are produced from one unit of the primary resource). Equations 2 and 3 constitute the basic Michaelis–Menten dynamics for bacterial growth on a single limiting resource in a chemostat (Edelstein-Keshet 1989).

I now extend this model to cross-feeding by assuming that bacteria secrete a secondary nutrient, here acetate, into the chemostat as a metabolic waste product of glucose consumption. Thus, the rate of production of this secondary nutrient is proportional to the glucose consumption rate  $\frac{1}{y_g} \frac{r_g \cdot c}{k_g + c} \cdot n$ . At the same time, the secondary nutrient is also consumed by the bacteria, with different parameters describing uptake efficiency. If  $a(t)$  denotes the concentration of the secondary nutrient in the chemostat at time  $t$ , the bacterial growth rate therefore becomes

$$\frac{dn}{dt} = \frac{r_g \cdot c}{k_g + c} \cdot n + \frac{r_a \cdot a}{k_a + a} \cdot n - d \cdot n \quad (4)$$

where  $r_a$  and  $k_a$  are Michaelis–Menten constants describing bacterial growth due to consumption of the secondary nutrient. The assumption underlying this equation is that uptake of the two resources is decoupled, so that waste products are first secreted into the medium and are subsequently consumed in a secondary metabolic pathway. It has been

argued that Eq. 4 is an appropriate model for bacterial growth on two different resources in a chemostat (Stewart and Levin 1973; Gottschal and Thingstad 1982).

Uptake of the secondary resource results in a decrease of its concentration, and taking the rate of production and the rate of loss due to outflow into account, the rate of change of  $a(t)$  becomes

$$\frac{da}{dt} = -\frac{1}{y_a} \frac{r_a \cdot a}{k_a + a} \cdot n - d \cdot a + \frac{e}{y_g} \frac{r_g \cdot c}{k_g + c} \cdot n \quad (5)$$

Here  $y_a$  is the yield for growth on acetate, and  $e$  is a constant of proportionality describing how glucose metabolism translates into production of the secondary nutrient. Because glucose uptake is not directly affected by the production of the secondary nutrient, the dynamic equation for the glucose concentration remains the same, and Eqs. 3–5 therefore describe bacterial growth on a primary resource in a chemostat with the addition of bacterial growth due to production of a secondary nutrient during consumption of the primary resource.

Before we formulate the evolutionary dynamics emerging from this ecological setup, we must specify which of the parameters in the ecological model should be viewed as phenotypic properties and which parameters should be regarded as nonevolving, externally fixed quantities. For consumption of a single resource without production of a secondary nutrient, i.e., for the situation described by Eqs. 2 and 3, it is known that coexistence of different bacterial strains is not possible. Instead, if we consider the compound parameter  $J = k_g d / (r_g - d)$ , which is the equilibrium concentration of the primary resource in the absence of cross-feeding, then in a mixture of strains the strain with the lowest  $J$  value will outcompete all other strains (Stewart and Levin 1973; Hanson and Hubbell 1980). In particular, in a mixture of strains with equal  $k_g$  values, the strain with the highest maximal growth rate  $r_g$  outcompetes strains with lower  $r_g$ . Note that coexistence of two strains is possible in competition in serial batch if both the  $r_g$  values and the  $k_g$  values are different and ranked in reverse order in the two strains (Stewart and Levin 1973). We discuss batch culture models at the end of this section, but for now we concentrate on chemostat cultures, and for simplicity we single out the maximal growth rates  $r_g$  and  $r_a$  as evolvable traits and consider all other quantities as fixed parameters. In particular, a glucose specialist has a high  $r_g$  and a low  $r_a$ , and vice versa for the acetate specialist. We note that the parameter  $e$ , determining how much waste acetate is secreted during glucose metabolism, is likely also an evolving trait, so that  $e$  is higher, i.e., acetate production increased, in strains that are more specialized on glucose (that is, these strains are very efficient at glucose uptake, but they also produce a lot of waste during glucose metabolism; Rosenzweig et al. 1994). However, to keep things simple I do not consider this quantity as a phenotypic trait in this article, and instead it will be considered, together with the other quantities  $k_g$ ,  $k_a$ ,  $y_g$ , and  $y_a$ , as an external parameter (note that these parameters may nevertheless influence the evolutionary dynamics).

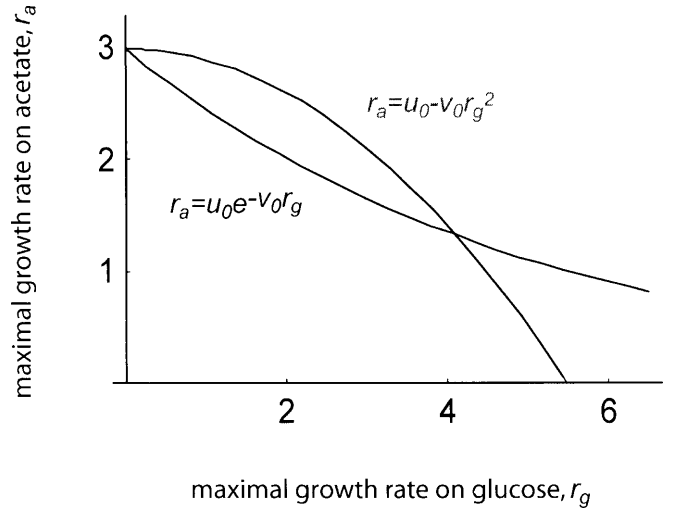


**Fig. 1.** Possible trade-off curves  $r_a = g(r_g)$  between maximal growth rate on glucose,  $r_g$ , and maximal growth rate on acetate,  $r_a$ . Shown are the functions  $r_a = u_0 - v_0 r_g^2$  with  $u_0 = 3$  and  $v_0 = 0.1$ , and  $r_a = u_0 \exp[-v_0 r_g]$  with  $u_0 = 3$  and  $v_0 = 0.2$ . Note that for the latter  $g' < 0$  and  $g'' > 0$  for all  $r_g > 0$ , whereas for the former  $g' < 0$  and  $g'' < 0$  for all  $r_g > 0$  (note that the biologically feasible range of  $r_g$  is bounded by the condition  $g(r_g) \geq 0$ )

Thus, the two traits whose evolution is to be studied are  $r_g$  and  $r_a$ , and to study the evolution of cross-feeding I assume that there is a trade-off between these two traits that constrains all possible phenotypes to a one-dimensional set in the two-dimensional  $r_g$ - $r_a$  plane. Specifically, I assume that there is a negative trade-off of the form

$$r_a = g(r_g) \quad (6)$$

such that  $g'(r_g) < 0$  (Fig. 1). Thus, the phenotypic value of  $r_a$  is uniquely determined by the value of  $r_g$  (and vice versa). Under these assumptions, the task is to study the adaptive dynamics of the trait  $r_g$ . To do this, we consider the growth rate of a rare mutant  $r'_g$  in an environment determined by the ecological dynamics of a resident population that is monomorphic for a resident phenotype  $r_g$ . If the ecological system given by Eqs. 3–5 is run to equilibrium for trait values  $r_g$  and  $r_a = g(r_g)$ , then the resulting equilibrium concentrations of glucose and acetate will be functions  $c^*(r_g)$  and  $a^*(r_g)$  of the resident phenotype. So long as the mutant is rare, it will not affect these concentrations. Therefore, the growth rate of the mutant population density  $n_{\text{mut}}(t)$  in the environment set by the resident will be

$$\frac{dn_{\text{mut}}}{dt} = \frac{r'_g \cdot c^*}{k_g + c^*} \cdot n_{\text{mut}} + \frac{r'_a \cdot a^*}{k_a + a^*} \cdot n_{\text{mut}} - d \cdot n_{\text{mut}} \quad (7)$$

where  $r'_g$  and  $r'_a = g(r'_g)$  are the phenotypes of the mutant, and where  $k_g$ ,  $k_a$ ,  $y_g$ ,  $y_a$ , and  $d$  are, as mentioned, fixed parameters.

Therefore, the per capita growth rate of the mutant  $r'_g$  in the resident  $r_g$ , which we denote by  $f(r'_g, r_g)$ , is given by

$$\begin{aligned}
f(r'_g, r_g) &= \frac{r'_g \cdot c^*(r_g)}{k_g + c^*(r_g)} + \frac{r'_g \cdot a^*(r_g)}{k_a + a^*(r_g)} - d \\
&= \frac{r'_g \cdot c^*(r_g)}{k_g + c^*(r_g)} + \frac{g(r'_g) \cdot a^*(r_g)}{k_a + a^*(r_g)} - d
\end{aligned} \tag{8}$$

where we have used the constraining relation  $r'_a = g(r'_g)$ . Based on the invasion fitness function  $f(r'_g, r_g)$ , we can define the selection gradient  $D(r_g)$  as

$$D(r_g) = \left. \frac{\partial f(r'_g, r_g)}{\partial r'_g} \right|_{r'_g = r_g} \tag{9}$$

According to the canonical equation of adaptive dynamics (Dieckmann and Law 1996), the evolutionary dynamics of the trait  $r_g$  is then given by

$$\frac{dr_g}{dt} = m \cdot D(r_g) \tag{10}$$

where  $m$  is a quantity that is determined by the mutational process and controls the speed of evolution. As we are only concerned here with qualitative features of the evolutionary dynamics of  $r_g$ , we can set  $m = 1$  without loss of generality.

Note that so long as  $D(r_g) < 0$ ,  $r_g$  will evolve to smaller values, while the contrary is true when  $D(r_g) > 0$ . Equilibrium points for the adaptive dynamics, which are also called evolutionarily singular points, are points  $r_g^*$  in phenotype space satisfying

$$D(r_g^*) = 0 \tag{11}$$

A singular point is an evolutionary attractor if

$$\frac{dD}{dr_g}(r_g^*) < 0 \tag{12}$$

for in that case selection tends to increase  $r_g$  if  $r_g < r_g^*$  and to decrease  $r_g$  if  $r_g > r_g^*$ , i.e., the evolutionary dynamics will converge toward  $r_g^*$ . An evolutionarily singular attractor  $r_g^*$  is called a branching point if  $r_g^*$  is a fitness minimum (Geritz et al. 1998), i.e., if

$$\left. \frac{\partial^2 f(r'_g, r_g)}{\partial^2 r'_g} \right|_{r'_g = r_g^*} > 0 \tag{13}$$

Thus, to find evolutionary branching points for the trait  $r_g$  we first have to solve Eq. 11 and then check whether inequalities 12 and 13 are satisfied. It follows from Eq. 9 that

$$D(r_g) = \frac{c^*(r_g)}{k_g + c^*(r_g)} + \frac{g'(r_g) \cdot a^*(r_g)}{k_a + a^*(r_g)} \tag{14}$$

Because  $g'(r_g) < 0$  by assumption, while all the other terms appearing in the last equation are  $> 0$ , it is possible that the equation  $D(r_g^*) = 0$  has a solution (note that this would not be possible if  $g' > 0$ ). However, it turns out that analytical

solutions are not feasible, due to the complexity of the expressions  $c^*(r_g)$  and  $a^*(r_g)$ ; in particular, it is also not feasible to determine analytically whether an evolutionarily singular point  $r_g^*$  is actually an attractor, i.e., whether Eq. 12 holds. These issues therefore have to be handled numerically by using pairwise invasion plots (Geritz et al. 1998), as is explained shortly.

First, let us note, however, that if an evolutionary singular attractor  $r_g^*$  exists, then the second derivative of the invasion function is given by

$$\left. \frac{\partial^2 f(r'_g, r_g)}{\partial^2 r'_g} \right|_{r'_g = r_g^*} = \frac{g''(r_g^*) \cdot a^*(r_g^*)}{k_a + a^*(r_g^*)} \tag{15}$$

Therefore, inequality 13 is satisfied if and only if  $g''(r_g^*) > 0$ , i.e., if and only if the trade-off curve between  $r_g$  and  $r_a$  has positive curvature at the singular point, as would necessarily be the case if  $g''(r_g) > 0$  independent of  $r_g$ , e.g., for trade-offs of the form

$$g(r_g) = u_0 \cdot \exp[-v_0 \cdot r_g] \tag{16}$$

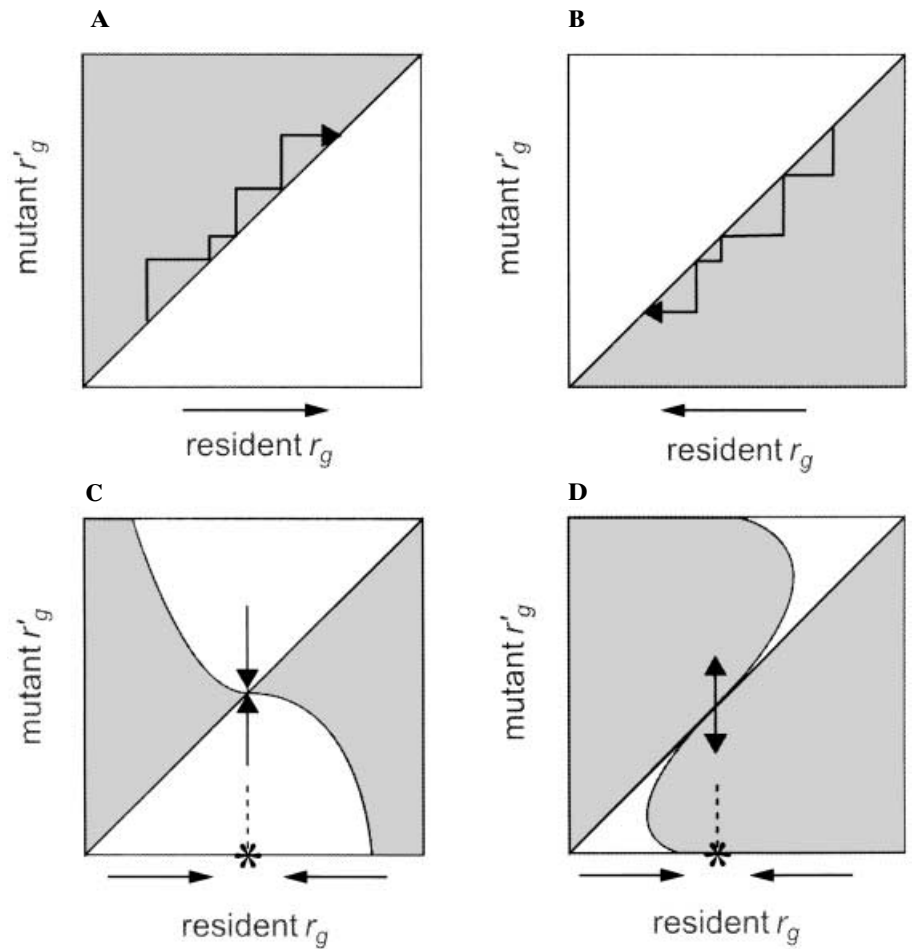
where  $u_0$  and  $v_0$  are parameters determining the exact shape of the trade-off (cf. Fig. 1). For our numerical results, we shall therefore consider trade-offs of the form of Eq. 16.

If analytical tools are lacking, a good alternative for determining the adaptive dynamics numerically consists of using pairwise invasion plots (Geritz et al. 1998), in which one plots, for each resident–mutant pair  $(r_g, r'_g)$ , the sign of the invasion fitness function  $f(r'_g, r_g)$ . Thus, in such plots the resident trait value is on the  $x$ -axis, the mutant trait value is on the  $y$ -axis, and a particular point  $(r_g, r'_g)$  is marked with a dot if  $f(r'_g, r_g) > 0$ , i.e., if the mutant  $r'_g$  can invade the resident  $r_g$ , and the point  $(r_g, r'_g)$  is left blank if  $f(r'_g, r_g) \leq 0$ , i.e., if the mutant  $r'_g$  cannot invade the resident. Note that by definition  $f(r_g, r_g) = 0$ , so that the diagonal is always blank.

If there is a range of resident  $r_g$  values for which a region adjacent to and above the diagonal consists of marked dots, and a region adjacent to and below the diagonal is blank, this implies that for each such resident mutants with slightly higher trait values can invade, whereas mutants with slightly lower trait values cannot invade. Thus, in such cases the trait value evolves to higher levels through a series of mutational steps, i.e., through a sequence of trait substitutions (Dieckmann and Law 1996), as indicated in Fig. 2A. A similar but opposite remark is true if there is region of resident  $r_g$  values for which the region adjacent to and above the diagonal is blank, while the region adjacent to and below the diagonal is marked (Fig. 2B).

Evolutionarily singular points are those points on the  $x$ -axis in a pairwise invasion plot at which the sign pattern of  $f(r'_g, r_g)$  across the diagonal changes (Geritz et al. 1998). In particular, evolutionary attracting singular points  $r_g^*$  are those points on the  $x$ -axis for which mutants with higher values than the resident are favored for residents with  $r_g < r_g^*$  (marked region above the diagonal for  $r_g < r_g^*$ ), while mutants with lower values than the resident are favored for

**Fig. 2.** Schematic illustration of various pairwise invasion plots. *Gray areas* consist of resident mutant pairs  $(r_g, r'_g)$  with  $f(r'_g, r_g) > 0$ , i.e., resident–mutant pairs for which the mutant can invade the resident (see text). **A** For all resident trait values,  $r_g$  mutants with  $r'_g > r_g$  have a positive growth rate whereas mutants with  $r'_g < r_g$  have a negative growth rate. Therefore, there is directional selection for larger trait values. The *arrow* indicates a series of trait substitutions, each of which is characterized by one vertical and the subsequent horizontal segment of the path; during each trait substitution, a mutant successfully invades (*vertical segment*) and becomes the new resident (*horizontal segment*), with the whole series of substitutions leading to an evolutionary increase in  $r_g$ . **B** Similar to **A**, but now with directional selection for small trait values. **C** A singular point is indicated by \* on the  $x$ -axis. To the right of \*, selection favors larger trait values (*gray area above diagonal*), and to the left of \* selection favors smaller trait values (*gray area below diagonal*). Therefore, \* is an evolutionary attractor. In addition, the *vertical line* through \* is outside the gray area; hence, \* is evolutionarily stable (no mutant can invade). **D** The singular point \* is an evolutionary attractor as in **C** but now the vertical line through \* lies entirely in the gray area, which means that all mutants can invade; therefore, \* is a fitness minimum, i.e., an evolutionary branching point



residents with  $r_g > r_g^*$  (marked region below the diagonal for  $r_g > r_g^*$ ). Two such situations are shown in Fig. 2C,D. In both cases, the point indicated by \* on the  $x$ -axis is a singular point attracting the evolutionary dynamics. In Fig. 2C, the vertical line passing through the singular point lies entirely in a blank region, which means that once the resident value is  $r_g^*$ , no mutant can invade. Therefore, this attractor for the adaptive dynamics is evolutionarily stable. In contrast, in Fig. 2D the vertical line passing through the singular attractor  $r_g^*$  lies entirely in a marked region, which means that every mutant can invade. In other words, in this situation  $r_g^*$  is actually a fitness minimum, and hence an evolutionary branching point. If, for a given set of parameters, the pairwise invasion plot looks like the one shown in Fig. 2D, then the trait  $r_g$  will first evolve to  $r_g^*$ , after which the population will become polymorphic and consist of two phenotypic branches that diverge evolutionarily from each other (see Geritz et al. 1998 for a complete theoretical treatment of evolutionary branching in one-dimensional trait spaces).

Therefore, in a numerical exploration we must look for pairwise invasion plots that look qualitatively like the one shown in Fig. 2D. The existence of such plots will imply the evolution of a cross-feeding polymorphism as envisaged in this article.

To conclude this section, I briefly mention how the model can be adapted to bacterial populations that are

propagated in serial batch cultures. Following Stewart and Levin (1973), the ecological model given by Eqs. 3–5 is changed by assuming a series of dynamic cycles representing the single batches. The dynamics for each single batch are obtained from Eqs. 3–5 by setting the parameter  $d = 0$  (no outflow), and by assuming the following initial conditions for the variables  $c$ ,  $n$ , and  $a$ :  $c(0) = c_0$  is set to some (high) initial value representing the initial concentration of glucose in the batch;  $n(0)$  is set to some small fraction of the endstate of the previous batch, representing the serial transfer of a small inoculate from the previous batch to the new batch, i.e.,  $n(0) = p \cdot n(t_{\text{end}})$ , where  $p$  denotes the fraction used for the inoculation and  $n(t_{\text{end}})$  is the bacterial population density at the end of the previous batch dynamics; finally,  $a(0) = 0$ , representing the fact that all glucose, and hence all secondary acetate, has been used up in the previous batch. With these initial conditions the dynamics are then again run to  $t_{\text{end}}$ , and the process of inoculation into a new batch is repeated. This iteration is done until  $n(t_{\text{end}})$  reaches an equilibrium, i.e., until  $n(t_{\text{end}})$  does not change further from one batch to the next.

The success of a mutant is then determined by assuming that the mutant is initially very rare, so that the ecological dynamics in a single batch of the quantities  $n(t)$ ,  $c(t)$ , and  $a(t)$ , where  $n(t)$  is the resident population density, are the same as just described, and the mutant dynamics in a single batch are simply determined by

$$\frac{dn_{\text{mut}}}{dt} = \frac{r'_g \cdot c}{k_g + c} \cdot n_{\text{mut}} + \frac{r'_a \cdot a}{k_a + a} \cdot n_{\text{mut}} \quad (17)$$

where  $r'_g$  and  $r'_a = g(r'_g)$  are the mutants trait values. (Note that this differs from Eq. 7, in which the nutrient concentrations are at their equilibrium values  $c^*$  and  $a^*$ ; here, these concentrations undergo the batch dynamics just described.)

Starting from a very small initial condition  $n_{\text{mut}}(0)$ , one calculates  $n_{\text{mut}}(t_{\text{end}})$  in the chemical environment determined by the dynamics of the resident during a single batch. The inoculate size of the mutant in the next batch is then  $p \cdot n_{\text{mut}}(t_{\text{end}})$ , and the mutant can invade, i.e., the invasion fitness  $f(r'_g, r_g) > 0$ , if and only if

$$\frac{n_{\text{mut}}(0)}{p \cdot n_{\text{mut}}(t_{\text{end}})} < 1 \quad (18)$$

By plotting the sign of the quantity  $1 - n_{\text{mut}}(0)/[pn_{\text{mut}}(t_{\text{end}})]$ , one can then construct pairwise invasion plots as before, from which one can deduce the adaptive dynamics of the trait  $r_g$  in a regime of serial batch cultures. As we will see in the next section, these dynamics are generally different from the evolutionary dynamics in models for chemostat cultures.

## Results

Recall that a central assumption in the adaptive dynamics model developed in the previous section is the trade-off  $r_a = g(r_g)$  between the maximal growth rates on the primary resource glucose,  $r_g$ , and the maximal growth rate on the secondary resource acetate,  $r_a$ . We assumed that this trade-off is of the form  $r_a = u_0 \exp[-v_0 r_g]$ , where  $u_0$  and  $v_0$  are parameters. For a given  $u_0$ , the parameter  $v_0$  determines the “severity” of the trade-off, i.e., how fast the value of  $r_a$  declines with an increase in  $r_g$ . Numerical simulations indicate that, depending on the rate  $e$  at which metabolized glucose is transformed into secondary acetate, the following two qualitatively different types of pairwise invasion plots represent typical evolutionary scenarios in the model so long as the severity of the trade-off is not too high, i.e., for low to moderate  $v_0$ .

If  $e$  is high enough, the invasion fitness function  $f(r'_g, r_g)$  constructed in the previous section yields pairwise invasion plots like the one shown in Fig. 3A. This plot shows the existence of two evolutionarily singular points, indicated by  $a$  and  $b$  on the  $x$ -axis. Here  $b$  is an evolutionary repeller, because for any  $r_g < b$  we have  $f(r'_g, r_g) > 0$  for  $r'_g < r_g$ , and for any  $r_g > b$  we have  $f(r'_g, r_g) > 0$  for  $r'_g > r_g$ . In other words, selection moves  $r_g$  away from  $b$  on both sides of  $b$ . Exactly the contrary is true for  $a$ : on both sides of  $a$ , selection drives  $r_g$  closer to the singular value (see magnification in Fig. 3B). Therefore,  $a$  is an evolutionary attractor. Moreover,  $a$  is a branching point, because  $f(r'_g, a) > 0$  for all mutants  $r'_g$  that are close to  $a$ . Thus, if the initial value of  $r_g$  at which the evolutionary process is started lies above  $b$ , then  $r_g$  will steadily increase over evolutionary time. However, if the

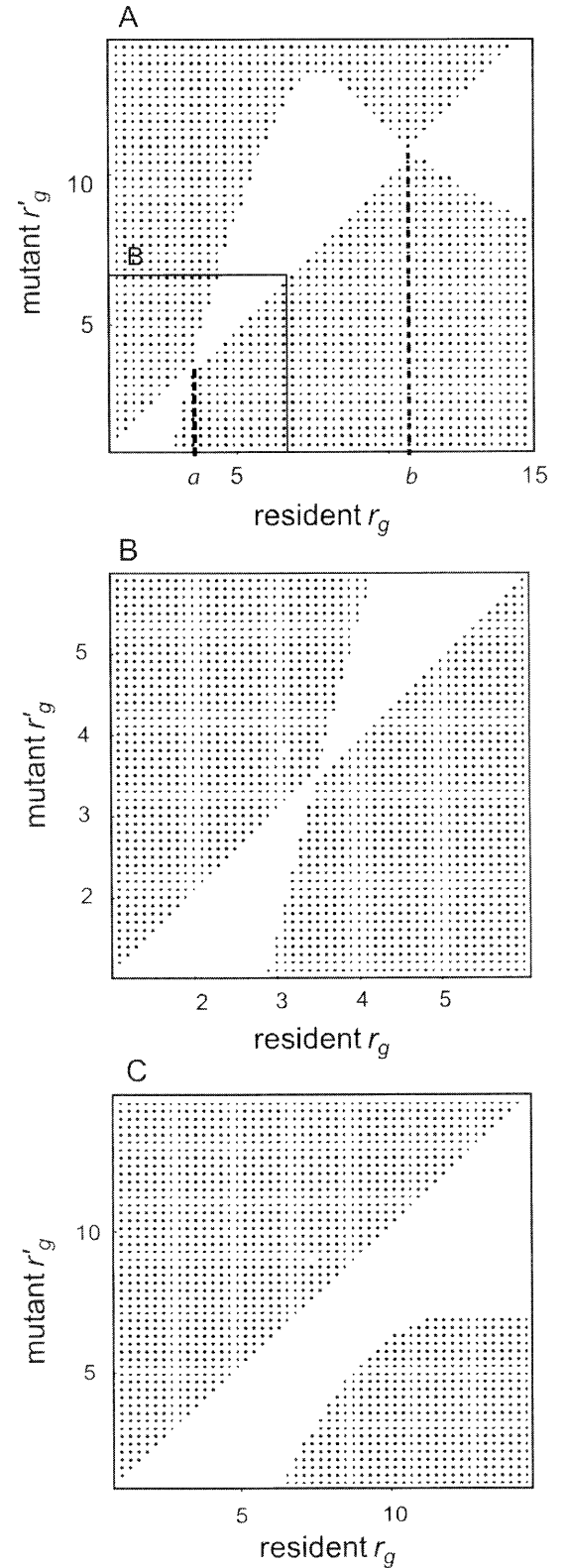


**Fig. 3.** Pairwise invasion plots for the evolution of cross-feeding. **A** Tradeoff  $r_a = u_0 \exp[-v_0 r_g]$  with  $u_0 = 3$  and  $v_0 = 0.2$  (this function is shown in Fig. 1). The pairwise invasion plot shows an evolutionary branching point ( $a$ ) and a repeller ( $b$ ). Parameter values:  $k_g = 1$ ,  $y_g = 1$ ,  $k_a = 1$ ,  $y_a = 1$ ,  $d = 1$ ,  $c_0 = 10$ ,  $e = 1.5$ . **B** Magnification of the *small square* indicated in **A**. **C** Here  $e = 0.5$ , i.e., there is less efficient conversion of glucose into acetate. The pairwise invasion plot shows that there is now uniform selection for larger  $r_g$  values

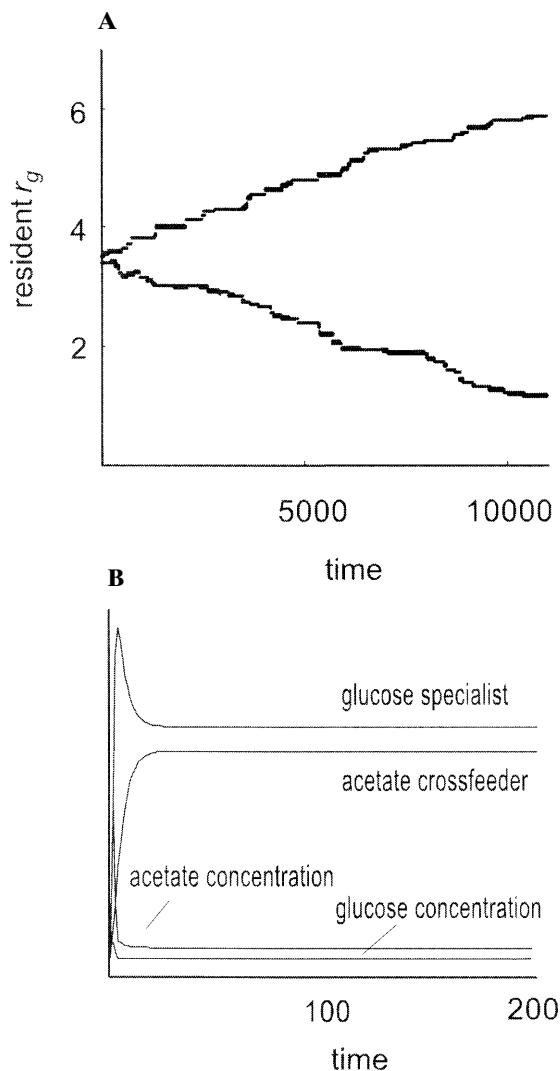


**Fig. 4. A** Evolutionary dynamics of a cross-feeding polymorphism after evolutionary branching. To simulate evolution in two coexisting strains, the basic ecological model 3–5 was extended in a straightforward way to competition between two bacterial strains. A given ecological system comprising two strains was first run to equilibrium, and then a mutant occurred with probability 0.1 in either strain. If a mutation occurred, its  $r_g$  value was chosen from a normal distribution with mean the resident  $r_g$  value and variance 5% of the mean. If the mutant had a positive growth rate on the equilibrium glucose and acetate concentrations determined by the two resident strains (which necessarily have zero growth rates on these concentrations, because they are at ecological equilibrium), then the mutant was assumed to replace the resident strain in which it appeared (otherwise the resident strain remained unchanged), and the new system was again run to ecological equilibrium. This process was started with two initial resident strains with  $r_g$  values that were very close to and on opposite sides of the branching point shown in Fig. 3B, representing a situation just after the initial polymorphism is established at the branching point. The figure illustrates diverging evolution in the two branches. Parameter values as for Fig. 3A. **B** Ecological dynamics of coexistence between glucose specialist and acetate cross-feeder. The two coexisting strains correspond to the polymorphism present at time  $t = 1000$  in **A**. One of the strains is a glucose specialist (high  $r_g = 5.78$ , low  $r_a = 0.94$ ), the other is an acetate cross-feeder (low  $r_g = 1.21$  and high  $r_a = 2.36$ ) (note that the y-axis does not have units because the absolute magnitude of densities and concentration is arbitrary)

initial value of  $r_g$  lies between 0 and  $b$ , then  $r_g$  will first converge to  $a$ , after which the population will become dimorphic. Figure 4 shows an example of the diverging evolutionary dynamics that occur after the population has converged to the branching point  $a$ . In one of the two branches  $r_g$  evolves to ever higher values, and in the other branch  $r_g$  evolves to ever lower values. In the example shown, both these processes would only stop because of externally imposed constraints on the range of physiologically possible efficiencies of resource uptake. What is clear, however, is that the evolving polymorphism consists of one phenotype with a high  $r_g$  and a correspondingly low  $r_a$ , representing a glucose specialist, and one phenotype with a low  $r_g$  and a correspondingly high  $r_a$ , representing an acetate specialist. Figure 4B shows the ecological dynamics of a coexisting pair consisting of a glucose specialist and an acetate cross-feeder. It is important to note that these coexisting specialists gradually evolved from a single ancestor through the process of evolutionary branching.

Technically speaking, the branching point  $a$  and the repeller  $b$  in Fig. 3A arise because the one-dimensional subset in the resident–mutant plane defined by  $f(r'_g, r_g) = 0$  has the shape carved out by the marked regions in Fig. 3A. This set consists of the diagonal [as  $f(r_g, r_g) = 0$  in any case], as well as of a second curve that arches across the diagonal before it bends back toward the  $x$ -axis, enclosing the blank area above the diagonal in the diagram. As the rate of production of acetate during glucose metabolism, given by  $e$ , is decreased, this blank area becomes smaller, until for small enough  $e$  the curved part of the set defined by  $f(r'_g, r_g) = 0$  no longer intersects the diagonal. If this is the case, the whole region above the diagonal is marked [i.e.,  $f(r'_g, r_g) > 0$  for any  $r'_g > r_g$ ], indicating that there is now uniform selection for increased  $r_g$  (cf. Fig. 2A). Note that for a range of intermediate resident  $r_g$  values there are mutants with lower  $r'_g$  values that can invade (as is indicated by the black region below the diagonal) and subsequently coexist with the resident (Fig. 3C). However, this can only occur if mutations toward lower  $r'_g$  values exceed a certain minimal size (which is given by the vertical distance between the current resident value and the black area below the diagonal). Such a scenario may still be relevant for cross-feeding polymorphism in real systems, where mutations may have large effects. Strictly speaking, however, this would not be evolutionary branching as defined in adaptive dynamics, because in the case shown in Fig. 3C diversification would not occur for arbitrarily small mutations.

The number of parameters in the model is quite large, and I have not fully explored the whole range of parameters. Note that it is possible to rescale the ecological equations 3–5 so that of the ten original parameters only six remain, two of which correspond to the two maximal growth rates, and the remaining four correspond, respectively, to the ratios  $y_g/y_a$ ,  $k_g/k_a$ ,  $c_0/k_g$ , and to  $e$ . Because the maximal growth rates are used in the trade-off, there are therefore four external parameters that can potentially affect the evolutionary dynamics resulting from a particular choice for the trade-off function. Numerical exploration indicate that none of the parameters  $y_g/y_a$ ,  $k_g/k_a$ , and  $c_0/k_g$



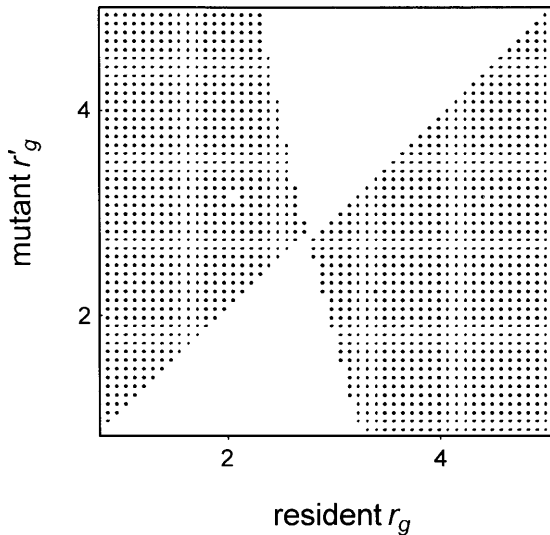


**Fig. 5.** Example of a pairwise invasion plot for the tradeoff  $r_a = u_0 - v_0 \cdot r_g^2$  with  $u_0 = 3$  and  $v_0 = 0.1$  shown in Fig. 1. In this case, an evolutionarily singular attractor  $r_g^*$  exists at which the tradeoff curve has negative curvature, i.e., with  $g''(r_g^*) < 0$  (cf. Fig. 1). Therefore, the evolutionary attractor is also evolutionarily stable (cf. Fig. 2C), and no evolutionary branching occurs. Other parameter values as in Fig. 3A

qualitatively affects the finding that a decrease in  $e$  results in the transition from Fig. 3A to 3C (so long as  $v_0$  is not too high). What is affected by changes in the external parameters, as well as by the parameter  $u_0$  in the trade-off function, is the point of transition between the two regimes. However, further and more detailed explorations may reveal regimes not reported here.

In particular, it is important to note that different trade-off functions can lead to different evolutionary dynamics. For example, as already noted (cf. Eq. 16), a trade-off function with negative curvature cannot lead to evolutionary branching, and instead often leads to the existence of an evolutionarily stable singular point  $r_g^*$ . If such a singular point is an attractor for the adaptive dynamics, an example of which is shown in Fig. 5, then it represents the final outcome of the evolutionary process, and branching, i.e., the evolution of a polymorphism, does not occur in such a model. This result reiterates the fact that positive curvature of the trade-off function at an evolutionarily singular point is a necessary condition for evolutionary branching.

To end this section, it is interesting to note that even with a trade-off with positive curvature, evolutionary branching seems to occur much less frequently in the evolutionary dynamics of populations that are propagated in serial batch cultures. For example, if the uptake parameters from Fig. 3A are used in the serial batch culture model, the pairwise invasion plot shown in Fig. 6A is obtained, in which the curved segment of the set  $f(r_g', r_g) = 0$  barely touches the diagonal. As mentioned, such cases can still give rise to the evolution of cross-feeding polymorphisms, especially if mutations have large effects. However, to obtain clear-cut cases of evolutionary branching in the serial batch culture

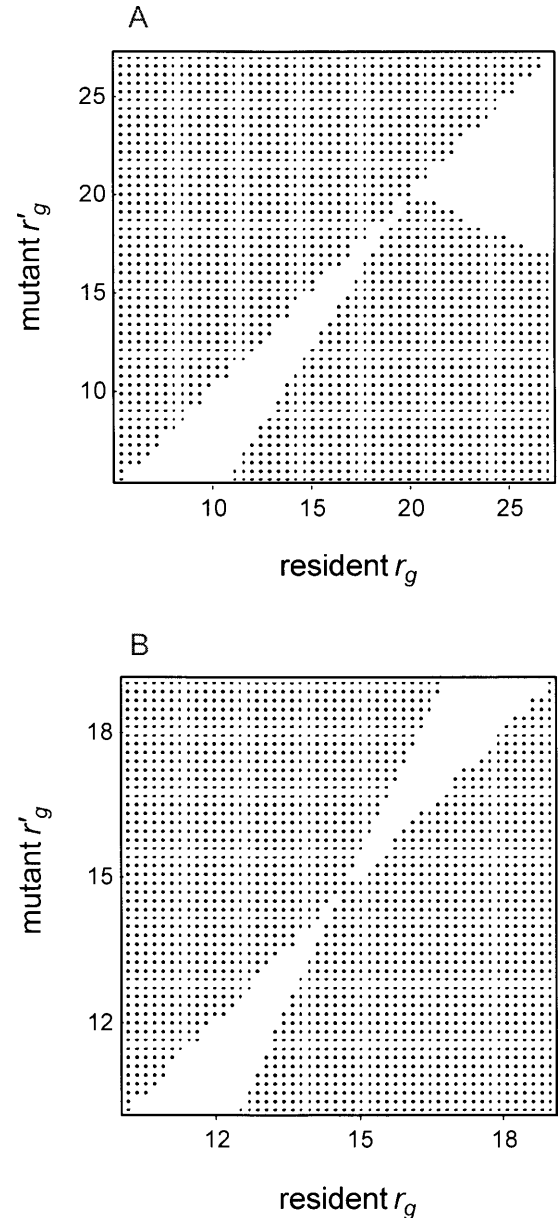


**Fig. 6.** Pairwise invasion plots for the serial batch culture model. **A** Same parameter values as in the chemostat model whose pairwise invasion plot is shown in Fig. 3A,B (note that the dilution rate  $d$  is not a parameter in the serial batch culture model, and  $c_0$  now denotes the initial glucose concentration in a single batch). The area above the diagonal is dark everywhere, indicating that mutants with higher trait values than the resident can always invade. There is also a dark area below the diagonal that touches the diagonal, indicating that for a range of resident values mutants with lower trait values can invade provided the difference between resident and mutant exceeds a certain threshold. The point on the  $x$ -axis above which the two dark areas below and above the diagonal come together is a fitness minimum, but it is not a branching point, because it is not an evolutionary attractor (to the right of this point, selection favors larger  $r_g$  values). **B** Evolutionary branching point in the serial batch culture model for higher conversion rate from glucose to acetate. The trade-off between maximal growth rates on glucose and acetate was of the form  $r_a = u_0 \exp[-v_0 r_g]$  with  $u_0 = 5$  and  $v_0 = 0.1$ ; other parameter values were  $k_g = 1$ ,  $y_g = 1$ ,  $k_a = 1$ ,  $y_a = 1$ ,  $c_0 = 10$  (initial glucose concentration in a single batch), and  $e = 5$

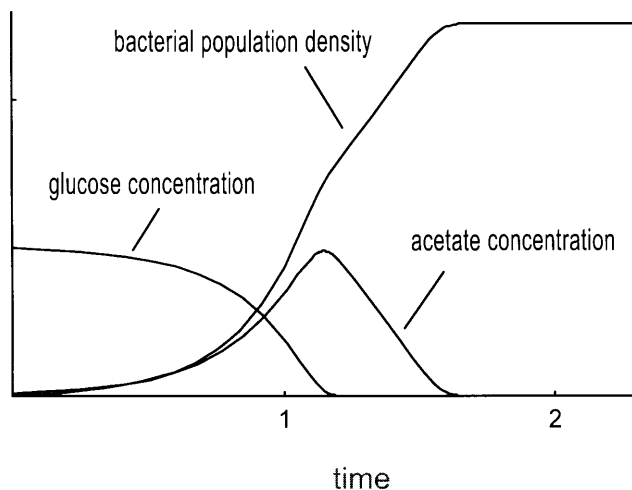


**Fig. 7.** Ecological dynamics of a bacterial population during a single batch of a serial batch culture (model as described in the text). Acetate has a significant concentration only for a relatively short period of time. Note that the bacterial population equilibrates because, for simplicity, no death is assumed to occur after all the glucose has been used up in the batch. Parameter values as for Fig. 6A. (Note that the y-axis does not have units because the absolute magnitude of densities and concentration is arbitrary)

models, the rate  $e$  at which acetate is produced from the glucose metabolism must be much higher. An example of an evolutionary branching point in serial batch culture is shown in Fig. 6B. Note that branching only occurs at a very high resident  $r_g$  value. Unfortunately, no analytical explanation is available at present why evolutionary branching occurs for a smaller range of parameters, and in particular requires higher conversion rates  $e$ , when bacterial populations are propagated in serial batch cultures. Nevertheless, Fig. 7 provides at least some intuitive arguments for this phenomenon. The figure shows the ecological dynamics of a monomorphic population and of the concentrations of the primary and secondary nutrients during a single batch. The concentration of the primary nutrient starts off at a high level and decreases to 0 as it is consumed by the bacteria, whose population eventually stops growing. The concentration of the secondary nutrient starts off at 0 in every single batch (as explained in the previous section), then increases due to metabolism of the primary resource, and then decreases again, due to consumption by the bacteria, as its production slows down because of a decrease in the consumption of the primary resource. Figure 7 illustrates that the period of time during which the secondary nutrient is at high concentrations is relatively short; this is in contrast to the conditions in the chemostat, where the concentration of the secondary nutrient attains a (positive) equilibrium state. This indicates that conditions for cross-feeders, i.e., specialists on the secondary resource, appear to be generally harsher in serial batch cultures than in chemostat cultures.

## Conclusions

The evolution of cross-feeding is one of the main empirical paradigms for evolutionary diversification and subsequent ecological coexistence of different microbial species on a single limiting resource. Various types of cross-feeding polymorphisms have been observed in the lab (Helling et al. 1987; Turner et al. 1996; Treves et al. 1998; Rozen and Lenski 2000), but the main mechanism appears to be that populations propagated from a single ancestral strain increase uptake efficiency on the primary resource, often glucose, which increases the amount of a secondary nutrient that results as a waste product of the metabolism of the primary resource. This in turn generates the conditions for a specialist on this secondary resource to be sustained, i.e., the conditions for the appearance of a cross-feeder. Although conditions for coexistence of different microbial species have attracted interest from theoreticians (Stewart and Levin 1973; Dykhuizen and Davies 1980; Gottschal and Thingstad 1982; Thingstad et al. 1996; Yomo et al. 1996), no theory appears to be available describing the gradual evolution of a monomorphic population into a cross-feeding polymorphism. The aim of the present article was to take the first step in filling this theoretical gap by applying the theoretical framework of adaptive dynamics to an idealized model for evolution in bacteria that are cultured on a single primary resource.

The model is based on an ecological description of the dynamics of a bacterial population consuming a primary resource that is continually supplied in a chemostat, as well as a secondary resource that is produced during consumption of the primary nutrient. The basic assumption I made is that there is a trade-off between uptake efficiencies on the two resources (see Fig. 1). Thus, a phenotype is characterized by a single trait, its uptake efficiency on the primary resource (or, alternatively, its uptake efficiency on the secondary resource, because the two efficiencies determine each other through the trade-off function). Because equilibrium concentrations of both the primary and the secondary resource depend on the phenotype of a given (monomorphic) resident population, the growth rate of a rare mutant also depends on which resident phenotype is present when the mutant appears. In other words, the growth rate of mutants is frequency-dependent, which sets the stage for evolutionary branching, a process by which a population first converges to a point in phenotype space at which selection turns disruptive due to frequency dependence, so that the population subsequently splits into two diverging phenotypic clusters representing the two resource specialists coexisting in a cross-feeding polymorphism (see Fig. 4).

Besides showing how a cross-feeding polymorphism can gradually evolve from a single ancestral strain through evolutionary branching caused by frequency-dependent selection, the theoretical analysis presented here makes two predictions. First, for cross-feeding to evolve in the models analyzed here, the trade-off between efficiencies in uptake of the primary and the secondary resource should have a positive curvature (at least at the singular point). Although

it is often difficult to measure the curvature of trade-offs, this prediction appears to be testable, e.g., by isolating strains at different times during an experiment that leads to the evolution of a cross-feeding polymorphism. In addition, if it were possible to manipulate trade-off curves experimentally (e.g., by using different types of media for bacterial growth), one could then test whether evolutionary branching becomes less likely when the curvature of trade-off curves becomes negative, as predicted by the model.

The second prediction of the model is that cross-feeding polymorphisms should be more likely in chemostat cultures than in serial batch culture, because in the models for the latter case evolutionary branching appears to require very high rates of production of the secondary nutrient during primary resource metabolism (see Fig. 6). This result conforms with some empirical data suggesting that, indeed, cross-feeding polymorphisms are less likely to be found in evolving bacterial populations that are propagated in serial batch cultures (Rozen and Lenski 2000). The suggested mechanism responsible for this is that in the single batches the concentration of the secondary nutrient is at appreciable levels only for a relatively short period of time, thus making conditions harsher for specialists on this secondary resource. Again, this is supported by the models presented here (see Fig. 7).

Clearly, however, these models are but a first step toward a more thorough understanding of the evolution of cross-feeding polymorphisms. Future work should include the analysis of alternative trade-offs, such as between the maximal growth rate  $r_g$  attained when the resource is not limiting and the “scavenging” growth rate  $k_g$  attained when the limiting resource is at very low concentrations (Hanson and Hubbell 1980), or trade-offs between efficiency  $e$  and yield  $y_g$  (Pfeiffer et al. 2001). In addition, it will be interesting to consider multiple waste products from the primary metabolism, which could result in the coexistence of multiple strains exhibiting various degrees of specialization on the different resources. For example, in addition to the glucose and acetate specialists, Rosenzweig et al. (1994) found a third bacterial species that cross-feeds also on glycerol, another waste product, and that exhibits properties of a generalist feeding on all three resources. In general, it is important to further reconcile theoretical results about the evolution of cross-feeding polymorphisms with empirical studies of this fundamental process of evolutionary diversification.

**Acknowledgments** I would like to thank Y. Toquenaga, M. Kawata and M. Shimada for their great hospitality, and M. Travisano for discussions.

## References

- Dieckmann U, Law R (1996) The dynamical theory of coevolution: a derivation from stochastic ecological processes. *J Math Biol* 34:579–612
- Dieckmann U, Doebeli M (1999) On the origin of species by sympatric speciation. *Nature (Lond)* 400:354–357
- Doebeli M, Dieckmann U (2000) Evolutionary branching and sympatric speciation caused by different types of ecological interactions. *Am Nat* 156:S77–S101
- Doebeli M, Ruxton GD (1997) Evolution of dispersal rates in metapopulation models: branching and cyclic dynamics in phenotype space. *Evolution* 51:1730–1741
- Dykhuizen D, Davies M (1980) An experimental model: bacterial specialization and generalists competing in chemostats. *Ecology* 61:1213–1227
- Edelstein-Keshet L (1989) *Mathematical models in biology*. McGraw-Hill, New York
- Geritz SAH, Kisdi E (2000) Adaptive dynamics in diploid, sexual populations and the evolution of reproductive isolation. *Proc R Soc Lond B* 267:1671–1678
- Geritz SAH, Kisdi E, Meszéna G, Metz JAJ (1998) Evolutionarily singular strategies and the adaptive growth and branching of the evolutionary tree. *Evol Ecol* 12:35–57
- Geritz SAH, van der Meijden E, Metz JAJ (1999) Evolutionary dynamics of seed size and seedling competitive ability. *Theor Popul Biol* 55:324–343
- Gottschal JC, Thingstad TF (1982) Mathematical description of competition between two and three bacterial species under dual substrate limitation in the chemostat: a comparison with experimental data. *Biotechnol Bioeng* 24:1403–1418
- Hansen SR, Hubbell SP (1980) Single-nutrient microbial competition: quantitative agreement between experimental and theoretical forecast outcomes. *Science* 207:1491–1493
- Helling RB, Varga CN, Adams J (1987). Evolution of *Escherichia coli* during growth in a constant environment. *Genetics* 116:349–358
- Jiggins CD, Naisbit RE, Coe RL, Mallet J (2001) Reproductive isolation caused by colour pattern mimicry. *Nature (Lond)* 411:302–305
- Kassen R, Buckling A, Bell G, Rainey PB (2000) Diversity peaks at intermediate productivity in a laboratory microcosm. *Nature (Lond)* 406:508–512
- Kisdi E (1999) Evolutionary branching under asymmetric competition. *J Theor Biol* 197:149–162
- Kisdi E, Geritz SAH (1999) Adaptive dynamics in allele space: evolution of genetic polymorphism by small mutations in a heterogeneous environment. *Evolution* 53:993–1008
- Maire N, Ackermann M, Doebeli M (2001) Evolutionary branching and the evolution of anisogamy. *Selection* 2:117–129
- Mayr E (1963) *Animal species and evolution*. Harvard University Press, Cambridge
- Metz JAJ, Geritz SAH, Meszéna G, Jacobs FJA, van Heerwaarden JS (1996) In van Strien SJ, Verduyn Lunel SM (eds) *Stochastic and spatial structures of dynamical systems*. North Holland, Amsterdam, pp 183–231
- Pfeiffer T, Schuster S, Bonhoeffer S (2001) Cooperation and competition in the evolution of ATP-producing pathways. *Science* 293:1436–1436
- Rainey PB, Travisano M (1998) Adaptive radiation in a heterogeneous environment. *Nature (Lond)* 394:69–72
- Rainey PB, Buckling A, Kassen R, Travisano M (2000) The emergence and maintenance of diversity: insights from experimental bacterial populations. *Trends Ecol Evol* 15:243–247
- Rosenzweig RF, Sharp RR, Treves DS, Adams J (1994) Microbial evolution in a simple unstructured environment: genetic differentiation in *Escherichia coli*. *Genetics* 137:903–917
- Rozen DE, Lenski RE (2000) Long-term experimental evolution in *Escherichia coli*. VIII. Dynamics of a balanced polymorphism. *Am Nat* 155:24–35
- Schliwien U, Rassmann K, Markmann M, Markert J, Kocher T, Tautz D (2001) Genetic and ecological divergence of a monophyletic cichlid species pair under fully sympatric conditions in Lake Ejagham, Cameroon. *Mol Ecol* 10:1471–1488
- Schluter D (1994) Experimental evidence that competition promotes divergence in adaptive radiation. *Science* 266:798–801
- Stewart FM, Levin BR (1973) Partitioning of resources and the outcome of interspecific competition: a model and some general considerations. *Am Nat* 107:171–198
- Thingstad TF, Havskum H, Garde K, Riemann B (1996) On the strategy of “eating your competitor”: a mathematical analysis of algal mixotrophy. *Ecology* 77:2108–2118

- Travisano M, Rainey PB (2000) Studies of adaptive radiation using model microbial systems. *Am Nat* 156:S35–S44
- Treves DS, Manning S, Adams J (1998) Repeated evolution of an acetate-cross-feeding polymorphism in long-term populations of *Escherichia coli*. *Mol Biol Evol* 15:789–797
- Turelli M, Barton NH, Coyne JA (2001) Theory and speciation. *Trends Ecol Evol* 16:330–343
- Turner PE, Souza V, Lenski RE (1996) Tests of ecological mechanisms promoting the stable coexistence of two bacterial genotypes. *Ecology* 77:2119–2129
- Via S (2001) Sympatric speciation in animals: the ugly duckling grows up. *Trends Ecol Evol* 16:381–390
- Xu W, Kashiwagi A, Yomo T, Urabe I (1996) Fate of a mutant emerging at the initial stage of evolution. *Res Popul Ecol* 38:231–237
- Yomo T, Xu W, Urabe I (1996) Mathematical model allowing the coexistence of closely related competitors at the initial stage of evolution. *Res Popul Ecol* 38:239–247